

# The $^{24}\text{Mg}(^3\text{He},t)$ reaction at 420 MeV.

R.G.T. Zegers,<sup>1,2,3,\*</sup> T. Adachi,<sup>4</sup> Sam M. Austin,<sup>1,3</sup> B.A. Brown,<sup>1,2,3</sup> Y. Fujita,<sup>5</sup> M. Fujiwara,<sup>4,6</sup> C. J. Guess,<sup>1,2,3</sup> H. Hashimoto,<sup>4</sup> K. Hatanaka,<sup>4</sup> M.E. Howard,<sup>3,7</sup> M. Matsubara,<sup>4</sup> R. Meharchand,<sup>1,2,3</sup> K. Nakanishi,<sup>4</sup> T. Ohta,<sup>4</sup> H. Okamura,<sup>4</sup> Y. Sakemi,<sup>4</sup> Y. Shimbara,<sup>1,3,†</sup> Y. Shimizu,<sup>4</sup> C. Scholl,<sup>8</sup> A. Signoracci,<sup>1,2</sup> Y. Tameshige,<sup>4</sup> A. Tamii,<sup>4</sup> and M. Yosoi<sup>4</sup>

<sup>1</sup>*National Superconducting Cyclotron Laboratory, Michigan State University, East Lansing, MI 48824-1321, USA*

<sup>2</sup>*Department of Physics and Astronomy, Michigan State University, East Lansing, MI 48824, USA*

<sup>3</sup>*Joint Institute for Nuclear Astrophysics, Michigan State University, East Lansing, MI 48824, USA*

<sup>4</sup>*Research Center for Nuclear Physics, Osaka University, Ibaraki, Osaka 567-0047, Japan*

<sup>5</sup>*Department of Physics, Osaka University, Toyonaka, Osaka 560-0043, Japan*

<sup>6</sup>*Kansai Photon Science Institute, Japan Atomic Energy Agency, Kizu, Kyoto 619-0215, Japan*

<sup>7</sup>*Department of Physics, The Ohio State University, Columbus, OH 43210, USA*

<sup>8</sup>*Institut für Kernphysik, Universität zu Köln, D-50937 Cologne, Germany*

(Dated: March 10, 2008)

The  $^{24}\text{Mg}(^3\text{He},t)$  reaction, populating states in  $^{24}\text{Al}$ , is studied at  $E(^3\text{He}) = 420$  MeV. By using a recently developed empirical relationship for the proportionality between Gamow-Teller strength and differential cross section at zero momentum transfer, such strengths to discrete levels in  $^{24}\text{Al}$  are extracted. In spite of a few small discrepancies for certain weak excitations, good consistencies with previous  $^{24}\text{Mg}(p,n)$  data and shell-model calculations using the USDA/B interactions in the *sd*-model space are found. Owing to the high energy resolution of 35 keV achieved, the locations of several energy levels in  $^{24}\text{Al}$  of importance for the estimation of the thermonuclear reaction rate of the  $^{23}\text{Mg}(p,\gamma)^{24}\text{Al}$  were determined. Results are consistent with two of the three previous  $(^3\text{He},t)$  measurements, performed at much lower beam energies. However, a new state at  $E_x(^{24}\text{Al})=2.605(10)$  MeV was found, corresponding to the third state above the capture threshold.

PACS numbers: 21.60.Cs, 25.40.Kv, 25.55.Kr, 26.30.-k, 27.30.+t

## I. INTRODUCTION

Charge-exchange (CE) reactions with hadronic probes provide an excellent tool to study the spin-isospin response in nuclei [1, 2]. A variety of CE probes has been employed, in particular to extract Gamow-Teller (GT;  $\Delta L = 0$ ,  $\Delta S = 1$ ,  $\Delta T = 1$ ) strength distributions. Since experimental studies of  $\beta$  decay only provide access to the response in a narrow energy window, CE studies have become the preferred way for mapping a more complete GT response.

The  $(^3\text{He},t)$  reaction at 420 MeV has been used extensively for extracting GT strengths in the  $\Delta T_z = -1$  direction (see e.g. Refs. [3–9]). Resolutions of as low as 20 keV in full-width at half-maximum (FWHM) have been achieved [10], providing a high level of detail for comparisons with theoretical calculations and allowing for a relatively clean extraction of GT strengths from transitions of different angular momentum transfer. In recent work [11] an empirical mass-dependent relationship for the proportionality between GT strength and differential cross section at zero momentum transfer (the so-called unit cross section) was established, similar to what had been done for the  $(p,n)$  reaction [12] about two decades

ago. This relationship is important for the extraction of GT strengths for cases where the unit cross section cannot be directly calibrated by using experimental  $\beta$  decay  $\log ft$  values. Such is the case for GT transitions from  $^{24}\text{Mg}$  into  $^{24}\text{Al}$  discussed here. The GT strength distribution in  $^{24}\text{Al}$  has been extracted in the past, by using the  $^{24}\text{Mg}(p,n)$  reaction at 135 MeV [13]. In that analysis, GT strengths had to be extracted by using the empirical relationship for the unit cross section specific for the  $(p,n)$  probe. A comparison between the  $(^3\text{He},t)$  and  $(p,n)$  results is thus a good check on the level of systematic errors made when employing such methods using different probes.

The accurate knowledge of the location of excited states of any spin parity in  $^{24}\text{Al}$  is important for the calculation of the thermonuclear reaction rate of  $^{23}\text{Mg}(p,\gamma)^{24}\text{Al}$  [14–18]. This reaction plays a significant role in explosive hydrogen-burning stars (e.g. novae) when the temperature is sufficiently high ( $0.1-2 \times 10^9$  K) for proton capture on  $^{23}\text{Mg}$  to compete with  $\beta$  decay. The total proton capture rate consists of a resonant contribution, due to unbound compound nuclear states, and a non-resonant direct-capture contribution. The resonant contributions depend exponentially on the resonance energies, which must thus be known with high accuracy. In the excitation energy region of relevance, just above the proton threshold (1.87 MeV) in  $^{24}\text{Al}$ , the available data on the resonance energies stems from three  $(^3\text{He},t)$  experiments performed at 81 MeV [19], 60 MeV [16] and 30 MeV [18]. Results from the latter two are consis-

\*Electronic address: zegers@nsl.msu.edu

†Current Address: Graduate School of Science and Technology, Niigata University, Niigata 950-2181, Japan

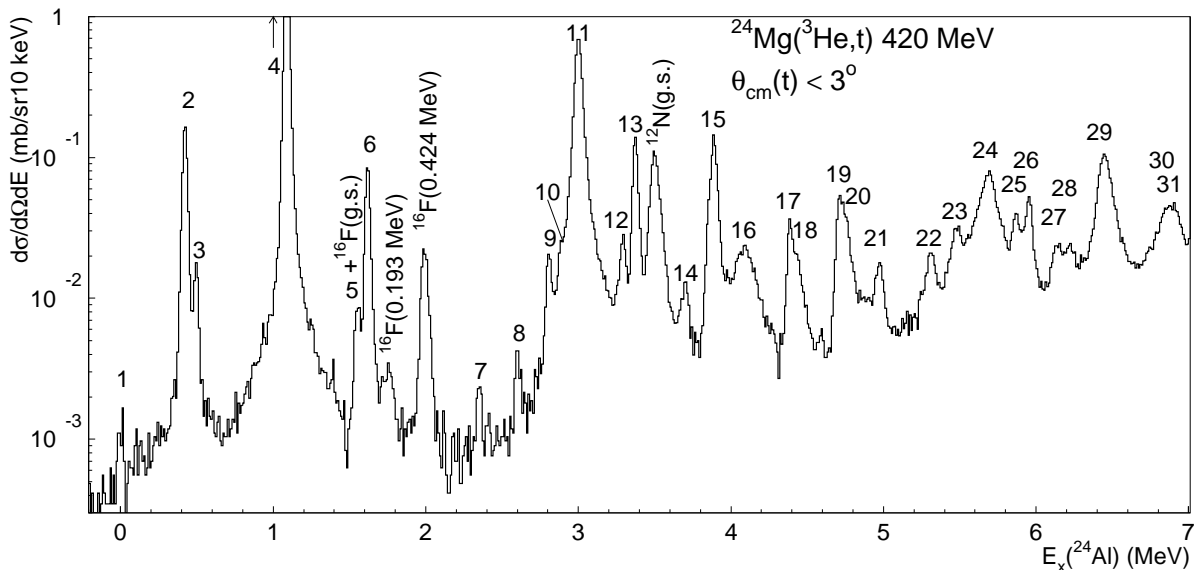


FIG. 1: Energy spectrum of the  $^{24}\text{Mg}(^3\text{He},t)$  reaction, integrated over the full opening angle used in the analysis. Peaks identified as excited states of  $^{24}\text{Al}$  are numbered. Peaks due to contaminants in the target are labeled as such. Note that the y-axis scale is logarithmic and that peak 4 extends beyond the maximum scale of the figure.

tent, but differ by about 30 – 50 keV from the results of Ref. [19]. In Ref. [17], resonance energies based on the then-adopted values [20] (averages of Refs. [16, 19]) were used to calculate the thermonuclear  $^{23}\text{Mg}(p,\gamma)^{24}\text{Al}$  reaction rates. In Ref. [18] newly measured resonance energies were used, leading to an increase in the proton capture rate of 5-20%, depending on the temperature. It is further to be noted that in the most recent compilation [21] (performed before the results from Ref. [18] became available) the adopted values were changed to those of Ref. [19]. In light of this history, an additional measurement of the relevant energies is desirable. Moreover, the current  $(^3\text{He},t)$  data are taken at much higher beam energies than the previous measurements and at very forward angles. Hence, the sensitivity for transitions with small angular momentum transfer is strongly increased compared to the experiments performed at the lower beam energies. This is important for checking the possible presence of resonances in the region just above the proton threshold, that have so far been undiscovered.

## II. EXPERIMENT AND DATA EXTRACTION.

The  $^{24}\text{Mg}(^3\text{He},t)$  experiment was performed at RCNP, by using a 420 MeV  $^3\text{He}^{2+}$  beam of  $\sim 15$  pA produced in the RCNP ring cyclotron. Scattered tritons from the  $^{24}\text{Mg}(^3\text{He},t)$  reaction on a 0.7-mg/cm<sup>2</sup> thick, 99.92% isotopically pure  $^{24}\text{Mg}$  target were momentum analyzed in the Grand Raiden spectrometer [22]. During storage and use in other experiments, the target had somewhat oxidized and also contained traces of  $^{12}\text{C}$ . However, these contaminants were useful for the energy calibration of the spectrum. An energy resolution of 35 keV (FWHM) was

achieved by using the lateral dispersion-matching technique [23]. The spectrometer was set at an angle of  $0^\circ$  and differential cross sections up to  $3^\circ$  in the center-of-mass could be extracted. To optimize the angular resolution, the angular dispersion matching technique was applied [23] and the experiment was run in over-focus mode [24, 25]. A resolution of  $0.2^\circ$  in laboratory scattering angle was achieved.

The  $^3\text{He}^{2+}$  beam was stopped in a Faraday cup, placed at the inside bend of the first dipole magnet of the spectrometer. The integrated current measured in the Faraday cup was used in the calculation of absolute differential cross sections. However, because of inefficient current integration when running in dispersion-matched mode, a correction had to be applied. To determine this correction factor, data were also taken on a  $^{26}\text{Mg}$  target (with a thickness of 0.87 mg/cm<sup>2</sup>), for which cross sections were available from the experiment in which the unit cross sections for extracting GT strength were calibrated [8, 11] and that was run in achromatic mode. It was found that a 20% correction to the cross sections had to be applied to the data taken in dispersion-matched mode. Except for this normalization factor, angular distributions for the  $^{26}\text{Mg}(^3\text{He},t)$  reaction measured in the current experiment and the experiment performed in achromatic mode were consistent. The spectrum from the  $^{26}\text{Mg}(^3\text{He},t)$  reaction was also useful for calibrating the triton energies measured in the spectrometer, since the excitation energy spectrum of  $^{26}\text{Al}$  is well known from two previous  $(^3\text{He},t)$  experiments [8, 26] and other experimental studies [20]. To do so, a minor correction had to be applied due to the small difference in thickness for the  $^{24}\text{Mg}$  and  $^{26}\text{Mg}$  targets. After this calibration, the uncertainties in the excitation energies of the  $^{24}\text{Al}$  spec-

trum were checked by using the  $^{24}\text{Al}$  ground state, the first excited state (at 0.4258(1) MeV; its location is well-known from a  $\gamma$  decay measurement [27]), two  $^{16}\text{F}$  states ( $E_x(^{16}\text{F})=0.193(6)$  MeV, 0.424(5)) and the  $^{12}\text{N}$  ground state. The deviations between the extracted and known values were 5 keV or less. Taking into account the small uncertainties when correcting the energies of reactions on different target nuclei due to recoil effects, the uncertainties in the excitation energies of the  $^{16}\text{F}$  excited states and possible higher-order magnetic field aberrations that affect the calibration, we assigned a minimum error of 10 KeV to all excitation energies in  $^{24}\text{Al}$  below 4 MeV. Above 4 MeV, the assigned energies becomes gradually more uncertain because there are few appropriate levels in the  $^{26}\text{Mg}(^3\text{He},t)$  spectrum to calibrate the triton energies with and no clear excitations stemming from reactions on contaminants in the  $^{24}\text{Mg}$  target present in the spectrum. Up to 5.5 MeV the assigned error was 20 keV and above that 30 keV. The statistical and systematic errors in the peak fitting procedure were mostly less than 3 keV, and thus minor compared to the errors in the energy calibration.

In Fig. 1 the energy spectrum of the  $^{24}\text{Mg}(^3\text{He},t)$  reaction is shown up to  $E_x(^{24}\text{Al})=7$  MeV. Most peaks are identified as excited states of  $^{24}\text{Al}$  and numbered. In certain cases, such as peak 10, which in Fig. 1 appears inseparable from peak 11, was identified only by inspecting the energy spectra at different scattering angles. Peaks due to the contaminants of rather different mass in the target were easily identified by studying the kinematic correlation between momentum and scattering angle of the triton associated with the recoil of the residual nucleus. Moreover,  $^{12}\text{C}(^3\text{He},t)$  and  $^{16}\text{O}(^3\text{He},t)$  spectra are well known, which was helpful to ensure that some of the broader states at higher excitation energies in  $^{24}\text{Al}$  were in fact not a result of reactions on these contaminants. Some of the  $^{24}\text{Al}$  states are only weakly populated, in particular states 7 and 8, which fall in the region of interest for the  $^{23}\text{Mg}(p,\gamma)^{24}\text{Al}$  reaction. Besides the fact that the dependence of the recoil energy on scattering angle for these states matched well with the expectation for a target with of mass of close to  $A=24$ , their energies also do not coincide with any known excitations in  $^{16}\text{F}$  or other possible contaminants. It is further noted that likely contaminants that might be present in trace amounts in the target and that are of similar mass as  $^{24}\text{Mg}$  and thus sustain similar recoil effects would have produced strong (i.e. much stronger than observed in peaks 7 and 8) signatures below the threshold of the  $^{24}\text{Mg}(^3\text{He},t)$  reaction ( $Q$  value of -13.987 MeV). The most probable background reactions,  $^{25}\text{Mg}(^3\text{He},t)$  and  $^{26}\text{Mg}(^3\text{He},t)$ , have  $Q$  values of -4.296 MeV and -4.023 MeV, respectively, and their spectra are well studied [8, 26, 28]. No significant signatures of these reactions were seen.

The data set was divided into five angular bins of  $0.5^\circ$  (laboratory angle) wide, and the yields for the peaks numbered in Fig. 1 obtained in each angular bin. If a peak was not isolated, the background under it was

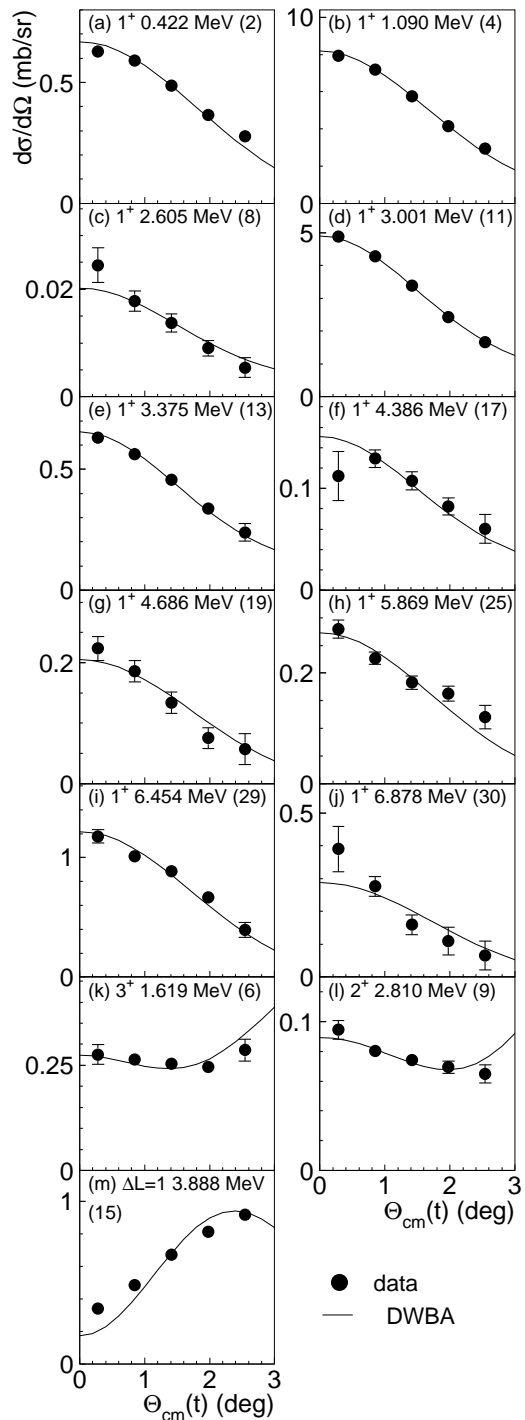


FIG. 2: Differential cross section for the  $^{24}\text{Mg}(^3\text{He},t)$  reaction at 420 MeV. (a-j) correspond to all transitions that were identified as GT. (k) corresponds to the excitation of the  $3^+$  state at 1.619 MeV, (l) corresponds to the excitation of the  $2^+$  state at 2.810 MeV and (m) corresponds to the excitation of a likely dipole state at 3.888 MeV (its multipolarity is uncertain). All experimental differential cross sections are compared with DWBA calculations which were scaled to the data in a single-parameter fit (see text). The numbers in brackets correspond to the labels for the peaks in Fig. 1.

parameterized with a polynomial in the energy region close to the peak and a systematic error to the yield was assigned based on the ambiguity in estimating the background. If two or more peaks were not separated, fits were performed simultaneously for those peaks and a background included in the fit, where necessary. By using the extracted yields, the differential cross sections in the center-of-mass system were calculated.

GT states were identified by using their typical strongly forward-peaked differential cross sections, associated with angular momentum transfer  $\Delta L = 0$ .<sup>1</sup> The differential cross sections of nearly all of the numbered states in Fig. 1 were compared with theoretical curves calculated in Distorted-Wave Born Approximation (DWBA) performed with the code FOLD [30]. The only exceptions were peaks 5 and 10, because the systematic errors in the extraction of the differential cross sections were too large. In those cases, we could only confirm that they do not strongly peak at forward angles and hence are not associated with a GT transitions. The DWBA calculations were very similar to those discussed in Ref. [8] where the  $^{26}\text{Mg}(^3\text{He},t)$  reaction at 420 MeV was studied and we refer to that paper for the details. The structure input for the DWBA calculations, in the form of one-body transition densities, was calculated using the *sd*-shell interaction USDA [31] in proton-neutron formalism (isospin-nonconserving) with the code OXBASH [32].

With the exception of peaks 5 and 10, all numbered peaks in Fig. 1 were compared with the DWBA calculation for a state of the best-matching multipolarity that was closest in excitation energy to the experimentally value. For each state, to compare the data with the theory, the DWBA calculations were scaled by an angle-independent factor that was determined in a fit. In Figs. 2(a-j), the comparison between the scaled DWBA calculations and the data are shown for all states identified as GT transitions. To illustrate that the angular distribution for GT transitions can be uniquely identified, the differential cross sections and matched DWBA calculations are shown for the transitions to the  $3^+$  state at 1.609 MeV (Fig. 2(k)) and the  $2^+$  state at 2.790 MeV Fig. 2(l). For both of these, the multipolarity is known [21]. In addition, the differential cross section for what is very likely a dipole transition at 3.862 MeV is shown in Fig. 2(m). The DWBA calculation shown in the plot assumes a transition to a  $2^-$  state. It was not possible to unambiguously assign the multipolarity for positive parity transitions with  $\Delta L > 0$  given the limited angular range available, and the same held for negative parity states of varying total angular momentum transfer. In the discussion below, the only distinction made is, there-

fore, between  $\Delta L = 0$  (GT) transitions and transitions with  $\Delta L \neq 0$ . It was not possible to unambiguously identify GT strength at excitation energies above 7 MeV in the spectrum, perhaps partially due to the limited angular coverage. Small amounts of GT strengths above 7 MeV were identified in the  $^{24}\text{Mg}(p,n)$  data [13] (see also below).

For the states that are identified as  $1^+$  states, the zero-degrees cross section was extracted from the fitted theoretical curve, with the uncertainty being deduced from the fitting error. To extract the GT strength ( $B(\text{GT})$ ) for each state by using the eikonal approximation [11, 12], requires the knowledge of the unit cross section ( $\hat{\sigma}$ ):

$$B(\text{GT}) = \frac{d\sigma}{d\Omega}(q=0)/\hat{\sigma}, \quad (1)$$

In addition, the differential cross sections at zero momentum transfer ( $q=0$ ) are needed. These were obtained by extrapolating the data at finite  $q$  (i.e. at finite  $Q$  value and  $0^\circ$  scattering angle) to  $q=0$  (i.e.  $Q=0$  and  $0^\circ$ ) by using the DWBA calculations:

$$\frac{d\sigma}{d\Omega}(q=0) = \left[ \frac{\frac{d\sigma}{d\Omega}(q=0)}{\frac{d\sigma}{d\Omega}(Q,0^\circ)} \right]_{\text{DWBA}} \times \left[ \frac{d\sigma}{d\Omega}(Q,0^\circ) \right]_{\text{exp}}. \quad (2)$$

In this equation, ‘DWBA’ refers to calculated values in the DWBA code. The unit cross section  $\hat{\sigma}$  was calculated with [11]:

$$\hat{\sigma} = 109 \times A^{-0.65}. \quad (3)$$

For the cases studied in Ref. [11], the error when using this equation was about 5%, except for certain transitions in which interference effects between  $\Delta L = 0$  and  $\Delta L = 2$  amplitudes to the excitation of  $J^\pi = 1^+$  GT states become strong. The  $\Delta L = 2$  contributions are mediated via the tensor- $\tau$  component of the effective nucleon-nucleon interaction [33, 34]. The errors associated with the interference were studied in detail in Refs. [8, 11, 35, 36]. Of most interest for the current study is the analysis in Ref. [8] for the  $^{26}\text{Mg}(^3\text{He},t)$  reaction. In a theoretical study based on the above-mentioned DWBA calculations using *sd*-shell one-body transition densities (with the USDB interaction) and the Love-Franey effective nucleon-nucleon interaction [33, 34], it was shown that errors associated with the interference between  $\Delta L = 0$  and  $\Delta L = 2$  amplitudes increase with decreasing values of  $B(\text{GT})$ . For  $B(\text{GT})=1, 0.1, 0.01$  and  $0.001$  the estimated errors were 3%, 11%, 20% and 28%, respectively (see Fig. 6 and Eq. (7) in Ref. [8]). An identical procedure for estimating the errors due to the tensor- $\tau$  interaction in the case of the  $^{24}\text{Mg}(^3\text{He},t)$  reaction was performed for the current work and very similar results were found. Since in the following, we will compare data from ( $^3\text{He},t$ ) and ( $p,n$ ) reactions, it should be noted that the tensor- $\tau$  interaction also introduces uncertainties for the latter [12]. However, as shown in Ref. [35] for the case of a  $^{58}\text{Ni}$  target, for a given transition, the effects of the interference are not

<sup>1</sup> Since  $^{24}\text{Mg}$  has  $N=Z$ , no excitation of the isobaric analog state ( $\Delta L = 0, \Delta S = 0$ ) is expected. A  $T = 2, 0^+$  state has been found at 5.957 MeV [29] but it cannot be excited in the  $\Delta T = 1$  ( $^3\text{He},t$ ) reaction on  $^{24}\text{Mg}$  ( $T = 0$ )

necessarily similar in magnitude for the  $(p, n)$  and  $({}^3\text{He}, t)$  reactions and even the sign of the interference can be different. Since it is hard to estimate the magnitude on a level-by-level basis, the uncertainties due to the tensor- $\tau$  interaction will not be quoted explicitly in the following section, but must be kept in mind when comparing data sets and checking the validity of theoretical calculations.

### III. RESULTS AND DISCUSSION.

#### A. GT strengths

In Table I, the results of the experiment are summarized and compared with previous results for the GT strength distribution extracted via the  ${}^{24}\text{Mg}(p, n)$  reaction at 135 MeV [13]. The listed uncertainties for the extracted GT strengths for both data sets stem from statistical and fitting errors only. For the current data, the combined error related to the uncertainty in the unit cross section (5%) and the uncertainty in the  ${}^{24}\text{Mg}$  target thickness was estimated to be 10%. The same value was given for the error in the extraction of the  $B(\text{GT})$  from the  $(p, n)$  data [13].

Overall a good correspondence between the GT strength from the current data and the  ${}^{24}\text{Mg}(p, n)$  data is found, but there are a few discrepancies. In Ref. [13] a  $1^+$  state was reported at 1.58 MeV, with a  $B(\text{GT})$  of 0.02, presumably corresponding to the state at 1.555 MeV (peak 5) in the current data. As mentioned above, we found that the angular distribution of this state is not associated with  $\Delta L = 0$ , although the analysis is complicated by the contamination from the  ${}^{16}\text{O}({}^3\text{He}, t){}^{16}\text{F}(\text{g.s.})$  reaction. However, even if this contamination is ignored and it is assumed that all events in this peak are due to a  $1^+$  state in  ${}^{24}\text{Al}$ , the  $B(\text{GT})$  would be 0.005. This upper limit is far below the value reported in Ref. [13]. It was, therefore, concluded that this is not a  $1^+$  state.

The  $1^+$  state found in the current data at 2.605 MeV (peak 8 in Fig. 1) was not seen in the  $(p, n)$  data, but that is understandable from the very small strength (0.0017(2)) associated with this excitation and the fact that the resolution in the  $(p, n)$  experiment was 310 keV, compared to the 35 keV reported here. Because the cross section for the excitation of this state is so small, one should worry about significant contributions from multistep processes even at the beam energy of 420 MeV. Such non-direct contributions can affect the angular distribution [37], and thus the identification of the state. Two other  $1^+$  states found in the current analysis were not seen in the  $(p, n)$  analysis, namely at 4.386 MeV and 5.869 MeV. These states likely correspond to  $1^+$  states measured at 4.40 MeV and 5.76 MeV in the measurement of  $\beta$ -delayed proton decay of  ${}^{24}\text{Si}$   $\beta$  [29] (Ref. [38] reports the former of these two at 4.38(5) MeV). Several of the other  $1^+$  states found in both the  $(p, n)$  and  $({}^3\text{He}, t)$  experiments correlate to  $1^+$  states found in those data, as indicated in Table I.

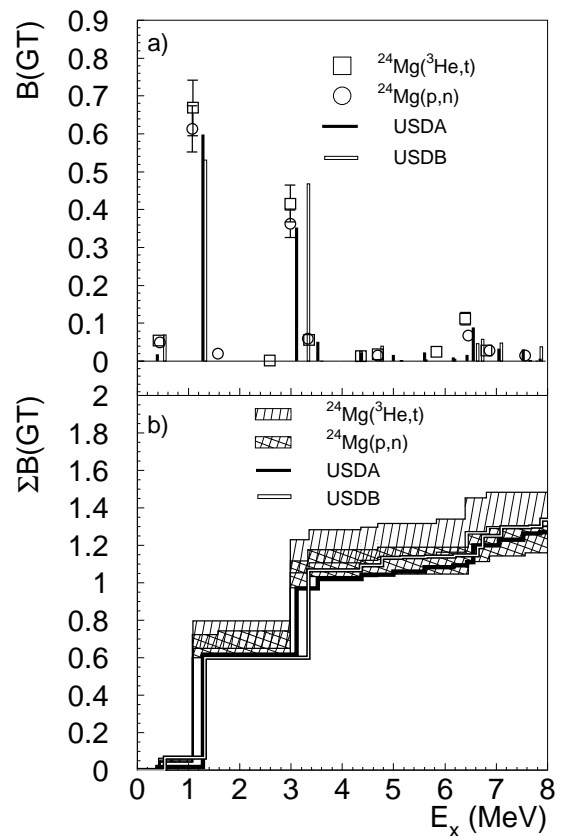


FIG. 3: (a) Comparison of GT strength distributions extracted from the current  ${}^{24}\text{Mg}({}^3\text{He}, t)$  data, the  ${}^{24}\text{Mg}(p, n)$  data [13] and calculated in shell-models using the USDA and USDB interactions [31]. (b) Cumulative sums of strengths for both data sets and theoretical calculations. The widths of the bands for the experimental results represent the uncertainties.

In Fig. 3(a), the extracted GT strengths from the  $(p, n)$  and current  $({}^3\text{He}, t)$  experiment are plotted, together with the results from shell-model calculations. The energy axis has been cut off at 8 MeV, but as shown in Table I, in the analysis of the  $(p, n)$  data small amounts of GT strength were detected up to about 11 MeV. For both data sets, the above mentioned uncertainties of 10% were used in combination with the statistical errors to calculate the total error bars. Besides the strength distribution calculated with the above-mentioned USDA interaction, the results using the USDB interaction [31] in the  $sd$ -shell model space are also shown. The difference between the USDA and USDB lies in the number of varied linear combinations of Hamiltonian parameters in the construction for each interaction; The USDA Hamiltonian was more constrained than the USDB Hamiltonian. Both theoretical calculations have been multiplied by a factor of 0.59 ([39–41] the error in this factor is 0.03), to take into account the quenching of the strength in the  $sd$ -shell due to a combination of configuration mixing with  $2p-2h$  states [42–44] and coupling to the  $\Delta(1232)$ -isobar nucleon-hole state [45]. Taking into account the uncer-

TABLE I: Overview of the results from the  $^{24}\text{Mg}(^3\text{He},t)$  experiment at 420 MeV (columns 1-5) and the comparison with  $^{24}\text{Mg}(p,n)$  results [13] for the extraction of GT strength (columns 6-7). In addition, results for the excitation energies from three  $^{24}\text{Mg}(^3\text{He},t)$  experiments at beam energies of 81 MeV [19], 60 MeV [16] and 30 MeV [18] are shown (columns 8-10) up and including to the region of interest for the  $^{23}\text{Mg}(p,\gamma)$  reaction at astrophysical temperatures.

$^{24}\text{Mg}(^3\text{He},t)$ present data					$^{24}\text{Mg}(p,n)$ [13]	$^{24}\text{Mg}(^3\text{He},t)$ [19]	$^{24}\text{Mg}(^3\text{He},t)$ [16]	$^{24}\text{Mg}(^3\text{He},t)$ [18]		
Fig. 1	$E_x(^{24}\text{Al})$	$\Delta L^a$	$d\sigma/d\Omega(0^\circ)^b$	$B(\text{GT})^{bc}$	$E_x(^{24}\text{Al})$	$B(\text{GT})^d$	$E_x(^{24}\text{Al})$	$E_x(^{24}\text{Al})$	$E_x(^{24}\text{Al})$	
label	(MeV)		(mb/sr)		(MeV)		(MeV)	(MeV)	(MeV)	
1	0	$\neq 0$	-	-			0	0		
2	0.422(10) <sup>e</sup>	0	0.67(1)	0.054(1)	0.44 <sup>e</sup>	0.050(1)	0.439(6) <sup>e</sup>	0.432(10) <sup>e</sup>		
3	0.492(10)	$\neq 0$	-	-			0.511(4)	0.506(10)		
4	1.090(10)	0	8.18(3)	0.668(3)	1.07	0.613(2)	1.111(3)	1.101(10)		
							1.275(5)	1.260(10)		
5	1.555(10)	$\neq 0$	-	<sup>f</sup>	1.58	0.020(6)	1.563(7)	1.535(10)	1.543(6)	
6	1.619(10)	$\neq 0$	-	-			1.638(8)	1.614(10)	1.619(6)	
7	2.349(10)	$\neq 0$	-	-			2.369(4)	2.328(10)	2.346(6)	
							2.546(7)	2.521(10)	2.524(6)	
8	2.605(10)	0	0.020(2)	0.0017(2)						
9	2.810(10)	$\neq 0$	-	-			2.823(6)	2.787(10)	2.792(6)	
10	2.89(20)	$\neq 0$	-	-			2.920(23)	2.876(10)	2.874(6)	
11	3.001(10) <sup>g</sup>	0	4.90(3)	0.416(3)	2.98	0.362(5)	3.037(16)	3.002(10)	2.978(6)	
									3.019(6)	
12	3.292(10)	$\neq 0$	-	-			...	...	...	
13	3.375(10) <sup>g</sup>	0	0.65(1)	0.056(1)	3.33	0.059(1)		additional states		
14	3.691(10)	$\neq 0$	-	-				not included in table		
15	3.888(10)	$\neq 0$	-	-						
16	4.088(50)	$\neq 0$	-	-						
17	4.386(20) <sup>g</sup>	0	0.15(1)	0.013(1)						
18	4.426(20)	$\neq 0$	-	-						
19	4.686(20) <sup>g</sup>	0	0.20(3)	0.018(3)	4.69	0.015(4)				
20	4.734(20)	$\neq 0$	-	-						
21	4.971(20)	$\neq 0$	-	-						
22	5.312(20)	$\neq 0$	-	-						
23	5.483(20)	$\neq 0$	-	-						
24	5.692(30)	$\neq 0$	-	-						
25	5.869(30) <sup>g</sup>	0	0.27(2)	0.024(2)						
26	5.952(30)	$\neq 0$	-	-						
27	6.141(30)	$\neq 0$	-	-						
28	6.214(30)	$\neq 0$	-	-						
29	6.454(30)	0	1.22(3)	0.112(3)	6.46	0.068(1)				
30	6.878(30)	0	0.3(1)	0.03(1)	6.87	0.029(1)				
31	6.896(30)	$\neq 0$	-	-						
				$\Sigma B(\text{GT})$	1.39(1)					
						> 7				
				$\Sigma B(\text{GT})$						1.216(9)
										0.084(9)
										1.300(13)

<sup>a</sup>All states which were not clearly related to  $\Delta L = 0$  transitions were assigned  $\Delta L \neq 0$ , even though in most cases a reasonable judgment on the angular momentum transfer can be made (see discussion in text).

<sup>b</sup>Errors are due to statistical and fitting uncertainties only.

<sup>c</sup> $B(\text{GT}) = \frac{d\sigma}{d\Omega}(q=0)/(109 \times (24)^{-0.65})$  (see text).

<sup>d</sup>Uncertainties are calculated from the error bars given in [13] for the differential cross sections at  $0^\circ$  and represent statistical and fitting uncertainties only.

<sup>e</sup>Corresponds to the 0.4258(1) state for which the energy is well known from  $\gamma$  decay [27].

<sup>f</sup>Upper limit for  $B(\text{GT})=0.005$ , assuming all events in this peak are due to a GT transition, ignoring possible contamination from the excitation of the  $^{16}\text{F}(\text{g.s.})$  and the non-matching angular distribution (see text).

<sup>g</sup>Likely corresponds to a  $1^+$  state observed in the  $\beta$ -delayed proton decay of  $^{24}\text{Si}$  [29] (see text).

tainties (including those due to the tensor- $\tau$  interaction, although they are not included in the plot), the two data sets and the theoretical calculations agree well. The calculation with the USDA interaction does slightly better in predicting the strength distribution than the USDB interaction. For example, with the USDA interaction the splitting of the GT strength into a strong and weaker state near 3.5 MeV matches well with the experimental results, whereas the calculation using the USDB interaction predicts a single  $1^+$  state in this region. At higher excitation energies, the USDA interaction also does slightly better in predicting the location of individual states. It is further noted that neither set of calculations predicts a  $1^+$  state near 2.5 MeV with small  $B(\text{GT})$  as observed in the current data.

In Fig. 3(b), the cumulative sums of GT strengths for the data sets and the theoretical calculations are shown. Slightly more strength is found in the present data, compared to the  $(p, n)$  results (see also Table I and the theory). However, taking into account the uncertainties, and in spite of the small discrepancies found for certain states, it can be concluded that the data sets match well and that both the theoretical calculations provide good description of the data.

### B. Excitation energies of low-lying states in $^{24}\text{Al}$

In the last three columns of Table I, the excitation energies found in the three  $^{24}\text{Mg}(^3\text{He}, t)$  experiments performed at beam energies of 81 MeV [19], 60 MeV [16] and 30 MeV [18] are given, up to energies ( $\sim 3$  MeV) of relevance for astrophysical applications mentioned in the introduction. Above 3 MeV, a state-by-state comparison between the low-energy data and the results from the current experiment becomes hard because of the increasing level density and the difference in sensitivities for transitions of various angular momentum transfers. Note that in the most recent low-energy experiment [18] energy levels below 1.5 MeV were not measured. As discussed in the introduction, there are significant differences between the three previous  $(^3\text{He}, t)$  measurements: the energy levels from Ref. [19] are inconsistent with those of Refs. [16, 18].

In Fig. 4, a comparison between the low-lying energy levels measured in the previous  $(^3\text{He}, t)$  experiments and the current data is made. The energies from the current experiment are chosen as reference (i.e. corresponding to 0 on the  $y$ -axis and providing the scale on the  $x$ -axis.) The following observations are made. The energy levels extracted in Ref. [19] are systematically higher than in the current data, by 15-20 keV, except for one state at 2.605 MeV. Ignoring that state for reasons discussed below, a  $\chi^2$  test for the consistency between the data from Ref. [19] and the current data showed that it is outside the 99% confidence interval ( $\chi^2 = 23.5$  with 9 degrees of freedom). Consistency tests between the current data and the data from Ref. [16] ( $\chi^2 = 9.46$  with 9 degrees

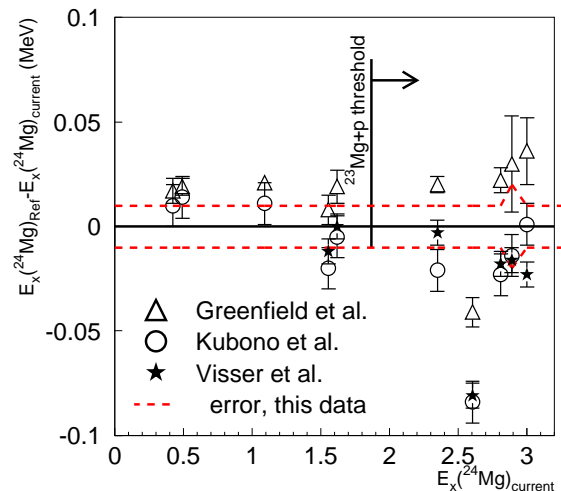


FIG. 4: Comparison between excitation energies found for low-lying states in  $^{24}\text{Al}$  for the  $(^3\text{He}, t)$  experiments by Greenfield et al. [19], Kubono et al. [16], Visser et al. [18] and the current data. The latter are taken as the reference and corresponds to a value of 0 on the  $y$ -axis. The dashed lines (color online) correspond to the error margins in the current experiment. The current data are also used for the  $x$ -axis scale, assuming the presence of a matched state in the other data. For the state at 2.605 MeV in the current data, this assumption appears to be incorrect, and points to the presence of a previously unknown state (see text).

of freedom) and Ref. [18] ( $\chi^2 = 7.98$  with 6 degrees of freedom) were well within the 95% confidence interval. If the calibration from Ref. [19] is therefore, rejected, the weighted average of the results for the first and most important excited state above the proton-capture threshold from Refs. [16, 18] and the current data is 2.343(5) MeV. This is consistent with the value used in Ref. [18] to calculate the proton-capture rate.

The state found in the current experiment at 2.605 MeV is  $\sim 80$  keV separated from its assumed counterparts ( $\sim 2.524$  MeV) in the works of Refs. [16, 18]. The deviation is less (40 keV) when comparing with the results from [19], but after taking into account that the energies in that data are systematically higher, it is almost equally inconsistent. We identified this as a  $1^+$  state (although somewhat uncertain, due to its small cross section and possible contributions from non-direct production mechanisms) based on its angular distribution, whereas the previous data suggests a multipolarity of  $4, 5^+$  [16, 19]. Transitions with large angular momentum transfer are relatively strongly excited in the low-energy experiment and strongly suppressed at 420 MeV (at forward scattering angles). On the other hand  $\Delta L = 0$  transitions are strongly enhanced at the higher energy and it could easily have been missed in the experiments at the lower beam energies. We, therefore, conclude that the state at 2.605 MeV seen in the current data is not the same as the state seen in the low-energy  $(^3\text{He}, t)$  data. Hence, it should be in principle be included

separately into the calculation of the  $^{23}\text{Mg}(p,\gamma)$  reaction rate as the third state above the capture threshold.

Unfortunately, since no  $1^+$  state is predicted near this excitation energy that is unaccounted for in the shell-model calculations, it is hard to make a reasonable calculation for the spectroscopic factor  $S$  (needed for calculating the proton partial width  $\Gamma_p$ ) and reduced  $\gamma$ -ray transition strengths (needed for calculating the  $\gamma$ -ray width  $\Gamma_\gamma$ ), as was done in [17] for other the other transitions. It is noted that in the shell model calculations presented in Table I of Ref. [17] a  $3^+$  state is predicted at 2.629 keV, but connected to an state experimentally observed at 2.900 MeV (Ref. [18] uses 2.874 MeV for this state). The calculations in Ref. [17] were performed with the original USD interaction [46]. The locations of the  $J^\pi = 1 - 5^+$  levels below 3 MeV as calculated with the USDA and USDB interactions [31] used in this work are consistent with the USD values to within 190 keV. The USDA(B) interaction situate this particular  $3^+$  state at 2.591 MeV (2.605 MeV). One can speculate that the new state at 2.605 MeV is in fact the  $3^+$  state predicted at that energy in the shell-model calculations and its measured angular distribution not consistent with that predicted in the one-step DWBA calculation as mentioned above. Based on this speculation, and following Ref. [17], we calculated  $\Gamma_\gamma$  and  $\Gamma_p$  in the shell model and deduced the resonance strength  $\omega\gamma = 10$  meV using the USDB interaction<sup>2</sup>. At a resonance energy of 0.734 MeV, the inclusion of this state would only change the proton-capture rate on  $^{23}\text{Mg}$  by maximally 2.5% at  $2 \times 10^9$  K, which is much smaller than other uncertainties in the rate given in Ref. [18]. The reason is that its resonance strength is much smaller than the strengths of the first two states above threshold. To do a more detailed and reliable calculation, confirmation of the existence and nature of the new state at 2.605 MeV in  $^{24}\text{Al}$  is desirable.

#### IV. CONCLUSION

We have measured the  $^{24}\text{Mg}(^3\text{He},t)$  reaction at 420 MeV and used the empirical relationship for the unit cross section as a function of mass number for this probe <sup>2</sup> Ref [17] used the original USD interaction [46] and found 12 meV

to extract the Gamow-Teller strengths for transitions to  $1^+$  states in  $^{24}\text{Al}$ . Owing to the high energy resolution achieved, several new small GT states have been discovered at energies below 7 MeV. Otherwise, taking into account the uncertainties involved with the extraction of GT strengths using fitted trends of unit cross section, the current ( $^3\text{He},t$ ) and previous ( $p,n$ ) experiments are in good agreement. The experimental results were also compared with theoretical calculations employing the USDA and USDB interactions and a satisfactory consistency was observed.

Because of the high energy resolution achieved, the energy of several levels of importance for estimating the proton capture rate on  $^{23}\text{Mg}$  for astrophysical purposes was studied. The results were consistent with two previous ( $^3\text{He},t$ ) experiments performed at beam energies of 60 MeV and 30 MeV, giving further indication that the values extracted from a third ( $^3\text{He},t$ ) experiment (at 81 MeV) are systematically too high. However, a new state is identified at 2.605(10) MeV, which is 0.734 MeV (and currently the third state) above the capture threshold. Based on the comparison with DWBA calculations, and from the fact that it was not observed in the low-energy experiments, we tentatively identified this state as having a multipolarity of  $1^+$ . This assignment is somewhat uncertain because of the small cross section and the associated possibility that non-direct contributions might have affected the angular distribution. Assuming it to be a  $3^+$  state, as predicted in shell-models, the proton-capture rates previously calculated are not strongly affected. However, more experimental information on this new state is needed to better judge the impact on the  $^{23}\text{Mg}(p,\gamma)$  reaction in stellar environments.

#### Acknowledgments

We thank the cyclotron staff at RCNP for their support during the experiment described in this paper. This work was supported by the US NSF (PHY0216783 (JINA), PHY-0555366, PHY-0606007), the Ministry of Education, Science, Sports and Culture of Japan and the DFG, under contract No. Br 799/12-1.

- 
- [1] M. N. Harakeh and A. van der Woude, *Giant Resonances: Fundamental High-Frequency Modes of Nuclear Excitations* (Oxford University Press, New York, 2001).
  - [2] F. Osterfeld, *Rev. Mod. Phys.* **64**, 491 (1992).
  - [3] M. Fujiwara *et al.*, *Nucl. Phys.* **A599**, 223c (1996).
  - [4] M. Fujiwara *et al.*, *Phys. Rev. Lett.* **85**, 4442 (2000).
  - [5] Y. Fujita *et al.*, *Phys. Rev. C* **70**, 054311 (2004).
  - [6] Y. Fujita *et al.*, *Phys. Rev. C* **70**, 011306(R) (2004).
  - [7] Y. Fujita *et al.*, *Phys. Rev. Lett.* **95**, 212501 (2005).
  - [8] R. G. T. Zegers *et al.*, *Phys. Rev. C* **74**, 024309 (2006).
  - [9] H. Fujita *et al.*, *Phys. Rev. C* **75**, 034310 (2007).
  - [10] Y. Fujita *et al.*, *Phys. Rev. C* **75**, 057305 (2007).
  - [11] R. G. T. Zegers *et al.*, *Phys. Rev. Lett.* **99**, 202501 (2007).
  - [12] T. D. Taddeucci *et al.*, *Nucl. Phys.* **A469**, 125 (1987).
  - [13] B. D. Anderson, N. Tamimi, A. R. Baldwin, M. Elaasar, R. Maday, D. M. Manley, M. Mostajabodda'vati, J. W. Watson, and W. M. Zhang, *Phys. Rev. C* **43**, 50 (1991).
  - [14] R. K. Wallace and S. E. Woosley, *Astrophys. J., Suppl. Ser.* **45**, 389 (1981).
  - [15] M. Wiescher, J. Görres, F.-K. Thielemann, and H. Ritter,



- Astron. Astrophys. **160**, 56 (1986).
- [16] S. Kubono, T. Kajino, and S. Kato, Nucl. Phys. **A588**, 521 (1995).
- [17] H. Herndl, M. Fantini, C. Iliadis, P. M. Endt, and H. Oberhummer, Phys. Rev. C **58**, 1798 (1998).
- [18] D. W. Visser, C. Wrede, J. A. Caggiano, J. A. Clark, C. Deibel, R. Lewis, A. Parikh, and P. D. Parker, Phys. Rev. C **76**, 065803 (2007).
- [19] M. B. Greenfield *et al.*, Nucl. Phys. **A524**, 228 (1991).
- [20] P. M. Endt, Nucl. Phys. **A633**, 1 (1998), and references therein.
- [21] R. B. Firestone, Nucl. Data. Sheets **108**, 2319 (2007), and references therein.
- [22] M. Fujiwara *et al.*, Nucl. Instrum. Meth. Phys. Res. A **422**, 484 (1999).
- [23] H. Fujita *et al.*, Nucl. Instrum. Methods Phys. Res. A **484**, 17 (2002).
- [24] H. Fujita *et al.*, Nucl. Instrum. Meth. Phys. Res. A **469**, 55 (2001).
- [25] R. G. T. Zegers *et al.*, Nucl. Phys. **A731**, 121 (2004).
- [26] Y. Fujita *et al.*, Phys. Rev. C **67**, 064312 (2003).
- [27] J. Honkanen, M. Kortelahti, J. Aysto, K. Eskola, and A. Hautajarvi, Phys. Scr. **19**, 239 (1979).
- [28] Y. Fujita, I. Hamamoto, H. Fujita, Y. Shimbara, T. Adachi, G. P. A. Berg, K. Fujita, K. Hatanaka, J. Kamiya, K. Nakanishi, et al., Phys. Rev. Lett. **92**, 062502 (2004).
- [29] V. Banerjee, T. Kubo, A. Chakrabarti, H. Sakurai, A. Bandyopadhyay, K. Morita, S. M. Lukyanov, K. Yoneda, H. Ogawa, and D. Beaumel, Phys. Rev. C **63**, 024307 (2001).
- [30] J. Cook and J. Carr (1988), computer program FOLD, Florida State University (unpublished), based on F. Petrovich and D. Stanley, Nucl. Phys. **A275**, 487 (1977), modified as described in J. Cook *et al.*, Phys. Rev. C **30**, 1538 (1984) and R. G. T. Zegers, S. Fracasso and G. Colò (2006), unpublished.
- [31] B. A. Brown and W. A. Richter, Phys. Rev. C **74**, 034315 (2006).
- [32] B. A. Brown *et al.*, NSCL report MSUCL-1289.
- [33] W. G. Love and M. A. Franey, Phys. Rev. C **24**, 1073 (1981).
- [34] M. A. Franey and W. G. Love, Phys. Rev. C **31**, 488 (1985).
- [35] A. L. Cole *et al.*, Phys. Rev. C **74**, 034333 (2006).
- [36] R. G. T. Zegers *et al.*, Phys. Rev. C **77**, 024307 (2008).
- [37] M. Igarashi, Phys. Lett. **B78**, 379 (1978).
- [38] S. Czajkowski *et al.*, Nucl. Phys. **A628**, 537 (1998).
- [39] B. H. Wildenthal, M. S. Curtin, and B. A. Brown, Phys. Rev. C **28**, 1343 (1983).
- [40] B. A. Brown and B. H. Wildenthal, Atomic Data Nuclear Data Tables **33**, 347 (1985).
- [41] B. A. Brown and B. H. Wildenthal, Annu. Rev. Nucl. Part. Sci. **38**, 29 (1988).
- [42] H. Hyuga, A. Arima, and K. Shimizu, Nucl. Phys. **A336**, 363 (1980).
- [43] A. Arima, Nucl. Phys. **A649**, 260c (1999).
- [44] K. Yako *et al.*, Phys. Lett. **B615**, 193 (2005).
- [45] M. Ericson, A. Figureau, and C. Thévenet, Phys. Lett. **B45**, 19 (1973).
- [46] B. H. Wildenthal, Prog. Part. Nucl. Phys. **11**, 5 (1984).